Surface & Coatings Technology 203 (2009) 3032–3036

Contents lists available at ScienceDirect

Surface & Coatings Technology

journal homepage: www.elsevier.com/locate/surfcoat

Characterization of hydrophobic and hydrophilic polythiophene–silver–copper thin film composites synthesized by DC glow discharges

J.C. Palacios [a,b,d,*], G.J. Cruz [c], M.G. Olayo [c], J.A. Chávez-Carvayar [a]

[a] Instituto de Investigaciones en Materiales, Universidad Nacional Autónoma de México, Circuito Exterior, Ciudad Universitaria, Apdo. Postal 70-360, Delegación Coyoacán, C.P. 04510, México
[b] Universidad Autónoma del Estado de México, Facultad de Ingeniería, Cerro de Coatepec, s/n Ciudad Universitaria, Toluca, C.P. 50130, México
[c] Departamento de Física, Instituto Nacional de Investigaciones Nucleares, Apdo. Postal 18-1027, Col. Escandón, D.F., C.P. 11801, México
[d] Universidad Politécnica del Valle de Toluca, Calle Loma Real s/n, Conjunto urbano La Loma, Zinacantepec, Estado de México, CP 51355, México

ARTICLE INFO

Article history:
Received 24 May 2008
Accepted in revised form 12 March 2009
Available online 18 March 2009

Keywords:
Plasma processing
Polymer–metal composites
Wettability
Polythiophene

ABSTRACT

Polythiophene with Ag and Cu particles were synthesized using DC glow discharges in order to study the transport properties and wetting behaviour of these polymer–metal composites. X-ray diffraction, scanning electron, transmission electron and atomic force microscopies were used to characterize the composites. The results indicated that the composites had nanotextures and microtextures with a thermally activated conduction mechanism at a low critical metallic volume fraction. The wetting behaviour of the composites varied from hydrophilic to highly hydrophobic as a function of the roughness and metallic content. In particular, the composites with a superficial nanotexture demonstrated a highly hydrophobic tendency.

1. Introduction

Polythiophene (PTh) has attracted considerable attention over the past years due to numerous solid state potential applications in many fields, such as microelectronic devices [1], catalysts [2], organic field effect transistors [3] and chemical sensors and biosensors [4,5]. For many years, the synthesis of PTh has been done mainly via electrolytic reactions due to the relatively high oxidative potential of thiophene that complicates its polymerization by other methods. However, in the last decade, the syntheses of PTh in gas phase by plasma have been acquiring importance due to the variety of possibilities that can be obtained. Maybe one of the most important is the formation of thin film composites with polymers, metals and different dopants with good adherence, branching, crosslinking and a high environmental and thermal stability [6,7]. One of the variables that can be partially manipulated in these syntheses is crosslinking, which can enhance the film strength as opposed to polymers formed by other methods.

Recent studies about the plasma polymerization have investigated the effect of power [8], dopants and humidity in the electrical conductivity of polypyrrole, polyaniline and polythiophene [6,9,10]. One disadvantage that has been observed in plasma polymerized PTh is that their electrical conductivity is lower than that of the semiconducting polymers synthesized by other methods. However, it has also been stated that the conductivity can be enhanced by adding metals to the polymers during the synthesis. This can be done releasing metallic atoms from the electrodes used to apply the electrical field in the reactor [11,12].

These polymer–metal composites can vary from insulators to conductors, depending on the metallic fraction. Conducting polymers may be good matrices for dispersing metallic particles, allowing an easy flow of electronic charges through the composites with a low ohmic drop. The size and distribution of these particles play an important role in the properties of the entire composite.

Another important factor is wettability, which has been less considered in these materials and that can be fundamental in a great number of possible applications. It is well known that this property is governed by both, roughness and chemical properties of the surfaces. Roughness and texturing have been studied in polypyrrole, polythiophene [6,10] and some of their metal–polymer composites [11] synthesized by plasma in order to manage the superficial energy in water repellent materials [13,14].

Now in this work, polythiophene with particles of Ag and Cu (PTh–Ag) were synthesized by DC glow discharges with the objective to study the effect of texture on the wettability of the composites. The syntheses started with thiophene in competitive cathode sputtering and polymerization. The characteristics of the electric field applied to the reactor promoted both processes simultaneously, which is difficult to obtain by other methods. In terms of wettability, the metal particles may increase the interaction of the surfaces with some liquids, which is studied in this work through their contact angles. The metallic percolation in the composites and the transport of charges are related

* Corresponding author. Facultad de Ingeniería, Universidad Autónoma del Estado de México, Cerro de Coatepec, s/n, Ciudad Universitaria, Toluca, CP 50130, México.
E-mail address: cuauhtemocpalacios@hotmail.com (J.C. Palacios).

0257-8972/$ – see front matter © 2009 Elsevier B.V. All rights reserved.
doi:10.1016/j.surfcoat.2009.03.020

in order to synthesize polymer–metal composites with controllable electrical conductivity and wettability for specific applications.

2. Synthesis

The glow discharges were carried out in a glass cylindrical reactor with stainless steel flanges and flat electrodes at each side, see Fig. 1. Both the flange and electrode of each side, were maintained at the same electrical potential. The anode was 65 mm diameter made of stainless steel and the cathode was 35 mm diameter made of a 90–10% Ag–Cu alloy. The distance between electrodes was 3 mm. A mechanical vacuum pump for corrosive gases Alcatel Pascal 2015C1 was used to reduce the pressure in the system. The electrodes were cleaned with water, soap and acetone before each synthesis.

Thiophene (Fluka, 98%) was introduced to the reactor in vapour phase. The monomer feed rate was regulated by a flow control valve. The electrical potential between the electrodes was applied with a power supply (MDX Advanced Energy magnetron drive) operated under constant voltage mode with the output power regulated at 800 V. In these conditions, part of the monomer feed was consumed in the polymerization and the other fraction was retained in a cold trap, cooled with liquid nitrogen, located between the reactor and the vacuum pump. The time of syntheses was in the 180–300 min interval. The total pressure inside the reactor was regulated between 0.3 and 0.5 mbar using air as a carrier gas. A flow control valve was used to let air enter into the reactor when low monomer feed rates were needed.

The polymers covered most of the internal walls of the reactor, but they concentrated in the area surrounding the electrodes. The front faces of the electrodes remained almost uncovered because of the continuous erosion during the syntheses. Lower film growth rates were obtained compared with those in other similar plasma polymer syntheses [6].

The composites were formed on glass substrates placed on the reactor walls at 3 cm from the electrodes, in the space between the electrodes and the negative flange. Most of the films were analyzed directly on glass substrates because their swelling was difficult to obtain with common solvents. However, the samples for transmission electron microscopy (TEM) analysis were carefully separated from the glass substrates. The swelling was a function of the metallic content in the polymers in which the samples with lower content swelled more easily than the others.

3. Characterization

The structure of the metal in PTh–Ag was studied by X-ray diffraction (XRD) with a Siemens D500 diffractometer. The scanned range was 2–120° 2θ, with a step of 0.02° and 1.2 s. The metallic volume fraction, x, and the metal distribution in the polymer matrix were studied by energy dispersive spectroscopy (EDS). A Leica-Cambridge (Stereoscan 440) scanning electron microscope (SEM) coupled with an EDS (Pentafet) microprobe and a JEM 1200EX

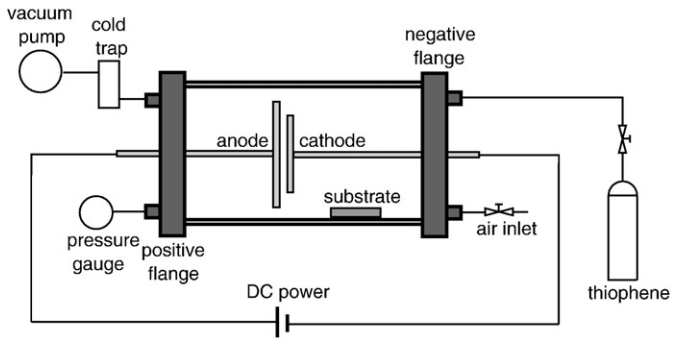

Fig. 1. Schematic representation of the reactor.

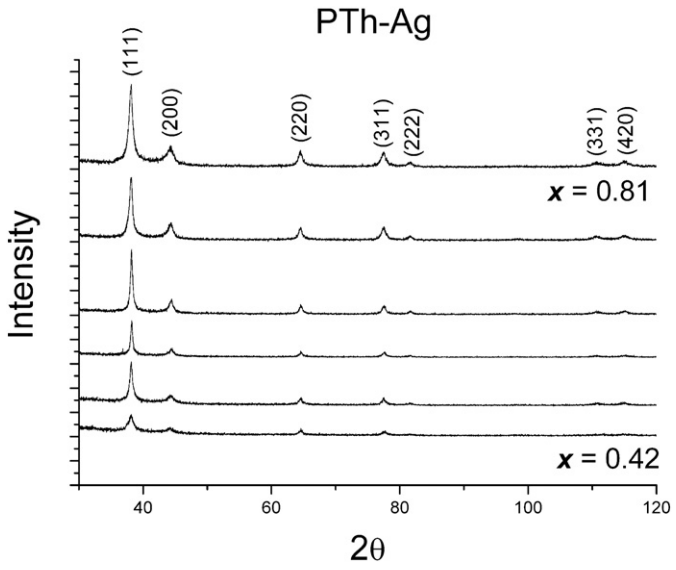

Fig. 2. XRD patterns of PTh–Ag composites with metal concentration from $x = 0.42$ to $x = 0.81$. Higher intensities are observed as x increases. The peaks correspond to cubic silver with preferred orientation of the (111) planes.

transmission electron microscope were used. The topography of PTh–Ag was studied by Atomic Force Microscopy (AFM) (JEOL JSPM-421) under atmospheric pressure conditions.

Contact angles between bidistilled water and the composites were measured at 37 °C by the Sessile drop method using a Rame-Hart Goniometer. The contact angles reported in this work, θ, are the average values obtained with drops of 8, 12 and 16 μL. At least 18 experiments were carried out for each case. The DC electrical conductivity of the composites was measured from 25 °C to 120 °C by the two-probe method.

4. Results and discussion

Thin films with thickness from 0.3 to 1.3 μm were obtained. The metallic volume fractions of Ag and Cu, x, were estimated using the density and the atomic fractions of the materials. Polymers with x from 0 to 0.81 were prepared. The XRD patterns of PTh–Ag with high metal concentration, from 0.42 to 0.81, are shown in Fig. 2. Higher intensities are observed as x increases. The peaks correspond to cubic silver, $a = 4.09$ Å, with the same structure as the cathode. Intense peaks in 38.1° and 44.2° 2θ are due to the (111) and (200) reflections. The intensity ratio between them can be associated to a preferred orientation of the (111) planes, as it has been observed in other polymer–metal composites synthesized by plasma [11].

As the XRD analyses are sensitive to the mass fraction of the components, which in this work is 90% Ag and 10% Cu, the more intense reflections of Cu in 43.4° and 50.5° are hidden by the Ag reflections. Consequently, the peaks of Cu are not perceptible, even in the upper pattern of Fig. 2. The elemental analysis of the metal particles also shows the same Ag/Cu ratio as the cathode. Unlike Ag/PTh composites prepared by other syntheses [15], no indication of chemical interaction between the metal and the PTh matrix was found in plasma PTh–Ag.

The SEM and TEM images in Fig. 3 show polymer matrices with metal particles of different sizes corresponding to composites with different x values. The structure of the composites is the result of many chemical and physical effects like reactivity, substrate temperature, etc. Two important factors in the synthesis are the competitive polymerization and metallic nucleation on the surfaces. The nucleation and growth of Ag particles highly depend on the average interatomic distance of the Ag atoms arriving to the substrate. Near the electrodes, high x values and large metal particles were observed.

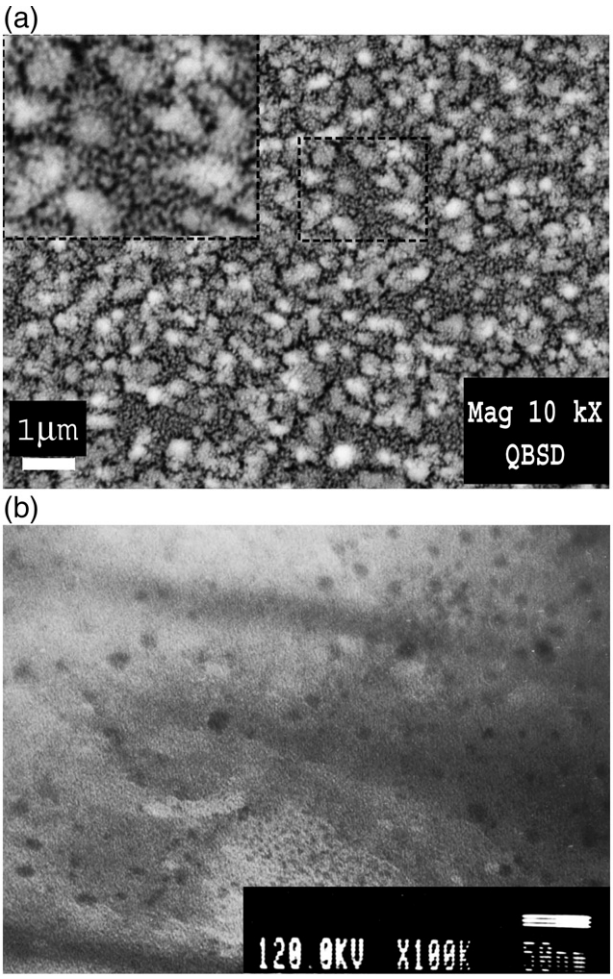

Fig. 3. Micrographs of PTh–Ag thin film composites with different x values. (a) SEM image. Metal particles with less than 1 μm diameter were found to be surrounded by smaller interconnected particles, $x=0.44$. (b) Metal nanoparticles, with sizes between 11 and 22 nm, with $x=0.07$, were observed by TEM.

Smaller metal particles appeared when the substrates were placed farther from the electrodes.

These results suggest that the polymerization inhibits the growth of metal particles. This effect can be explained if we consider that the probability to polymerize is almost the same in the entire synthesis region and that the composites are formed by condensation of oligomers and metallic atoms. Thus, as the metallic atoms travel within the reactor, the probability of being trapped in that environment of monomers, oligomers and constantly growing chains increases proportionally to the displacement.

The PTh–Ag composites studied in this work were synthesized 3 cm away from the cathode. Fig. 3a shows the surface of PTh–Ag with particles of less than 1 μm diameter, surrounded with smaller metal particles. If x is slightly diminished, smaller metal particles are formed. Fig. 3b shows the surface of PTh–Ag with metal nanoparticles in sizes between 11 and 22 nm. Under the described conditions, the competitive sputtering and polymerization on the electrodes strongly depends on the monomer feed rate.

The effective electrical conductivity was studied as x and temperature functions. Characteristic curves of electrical conductivity are shown in Fig. 4. Three electrical regimes can be observed: metallic, percolation and dielectric. At high metallic volume fractions, the metallic particles form continuous paths, see Fig. 3a, with polymer inclusions and metallic conduction. When the fraction of metallic particles reaches the threshold, x_p, a non-metallic transition occurs.

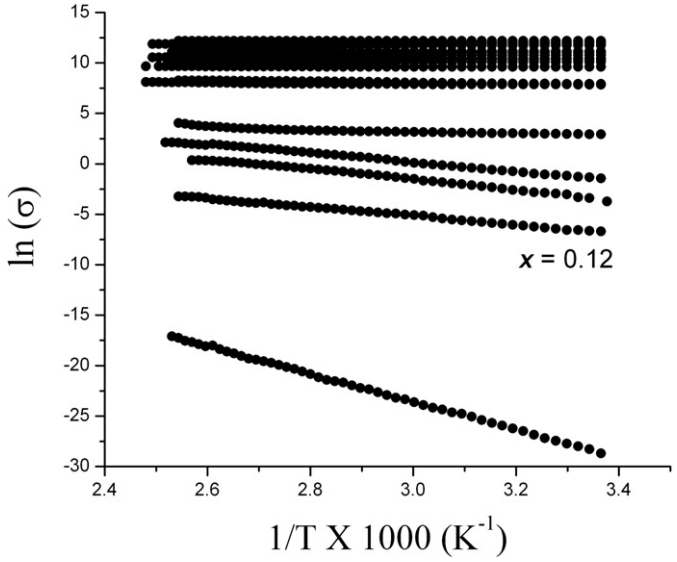

Fig. 4. Arrhenius behaviour of the electrical conductivity of PTh and PTh–Ag composites. The percolation threshold was observed at $x_p \approx 0.12$.

This has been explained before using percolation theories and geometrical approaches predicting x_p for 2D and 3D models [16]. In the dielectric regime, no continuous metal paths are observed, see Fig. 3b, and under low field conditions, the conductivity mechanism can be thermally activated. The work temperature range of the composites is limited by the temperature of degradation. For all the investigated temperature ranges, the DC conductivity can be fitted using the Arrhenius equation:

$$\sigma = \sigma_0 e^{-\frac{E_a}{kT}},$$

where E_a denotes the activation energy.

For the three conduction regimes, activation energies vs. x are plotted in Fig. 5. Activation energies from 1.2 eV, for $x=0$, to negative values were observed. An abrupt change in the slope of the curve can be observed at a low critical volume fraction, $x_c \approx 0.18$. From $x=0$ to $x=x_c$, the conductivity is visibly dependent on temperature which indicates a thermally activated conduction mechanism. At $x_o=0.30$,

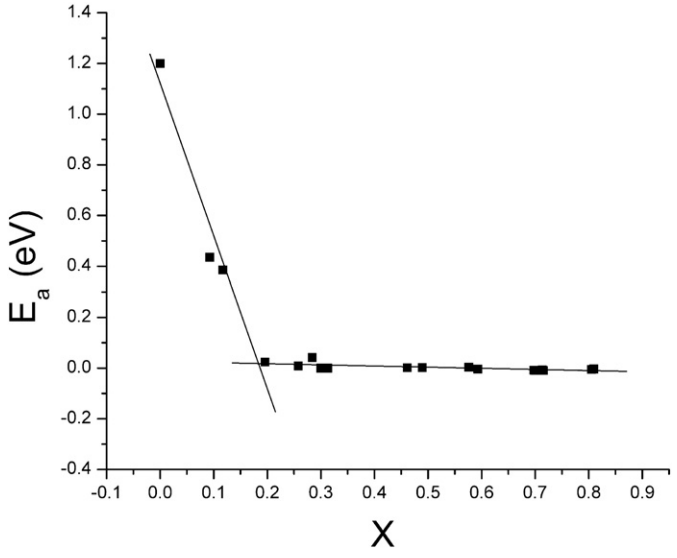

Fig. 5. Activation energy as a function of the metal volume fraction. An abrupt change in the slope is observed at $x_c \approx 0.18$. $E_a \approx 0$ for $x_o \approx 0.30$.

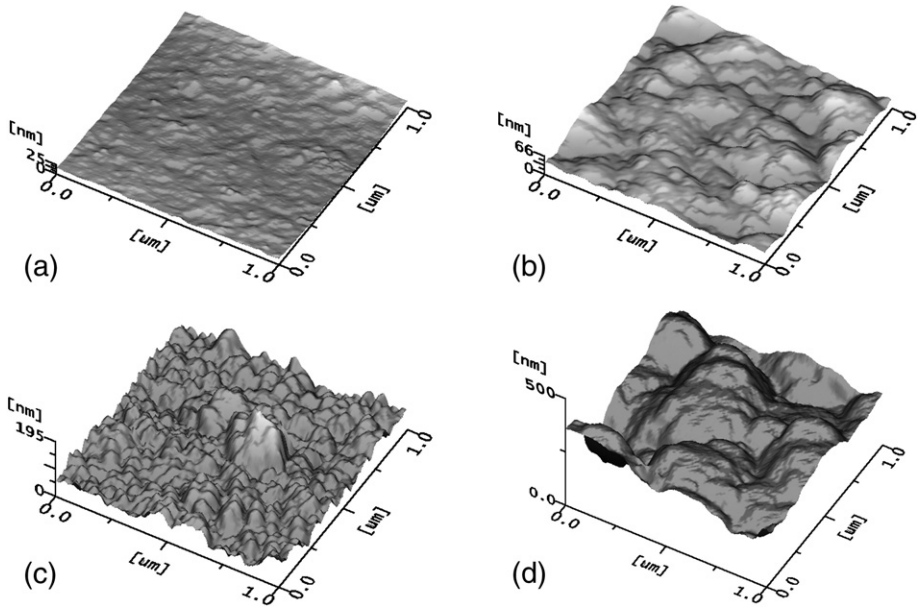

Fig. 6. AFM images of PTh and PTh–Ag surfaces. (a) PTh, $x=0$, Rrms = 4.1 nm, $\theta=29.7°$, (b) PTh–Ag, $x=0.22$, Rrms = 11.2 nm, $\theta=63.5°$, (c) PTh–Ag, $x=0.45$, Rrms = 23.2 nm, $\theta=120°$, (d) PTh–Ag, $x=0.69$, Rrms = 52.8 nm, $\theta=107°$.

the conductivity becomes entirely independent of the temperature, $E_a \approx 0$. The percolation threshold was observed at $x_p \approx 0.12$, where the conductivity changes in almost seven orders of magnitude. In all cases, x_p is lower than 0.4, a value found by Biederman [17] in metal–organic composites formed by plasma. Near x_p, the percolation theory predicts a relation between the conductivity and x_p, $\sigma \propto (x - x_p)^{\mu}$, where μ is a critical exponent, accepted as 1.3, for 2D systems [16].

Fitted results with the power law model indicated that the percolation threshold is 0.26. This value is also higher than the critical volume fraction observed in this work. The reason may be associated to a less considered factor in percolation models, such as the small size of the metallic particles. A recent 3D model developed by Xue [18] for ellipsoidal metal particles shows that the percolation threshold decreases quickly with the filler size. In this case, for $x<x_p$, metal nanoparticles with less than 22 nm diameter were found. Another factor not considered in percolation models, which can be associated with high conductivity changes is the thermally activated conductivity of the polymer matrix. Near x_p, the conduction mechanism of composites with aggregated nanoparticles is complex and may become low field induced. Small voltages applied to the samples can produce a very high internal electrical field between extremely close metal particles and would provide electrons with enough energy to escape from the metal by field emission, particularly if the particles are embedded in low resistance polymeric matrixes, as is the case with a semiconductive polymer. Kiesow [19], for example, reported an abrupt change in the current–voltage behavior for composites with aggregated nanoparticles in percolation structures when low voltages are applied between electrodes. In a large x range, from $x_0=0.30$ to $x=0.58$, the conductivity remains almost constant. For $x>0.58$, the temperature coefficient of electrical resistivity becomes positive, and the composites show metallic conductivity.

Fig. 6 shows AFM images of PTh and PTh–Ag surfaces in which smooth composites, Fig. 6(a), composites with nanotextures, Fig. 6(c), and composites with microtextures, Fig. 6(d), were observed. It was found that the roughness of PTh–Ag composites grows with x, and it can be separated in two intervals. In the first one, from 0 to ≈ 0.65, smooth surfaces (root mean square roughness Rrms<5 nm) and surfaces with nanotextures (protrusions less than 50 nm diameter and Rrms<25 nm) were observed. Roughness grows in a slightly proportional way to x, Fig. 7, from ~4 nm to ~24 nm (Rrms). In the second interval, $x>0.65$, roughness grows notably and surfaces with microtextures can be obtained, see Fig. 7.

The contact angles also increased almost linearly from 29.7° to 120° as x increases from 0 to 0.45, see Fig. 8. The most hydrophilic material of this work was the pure plasma polymer, PTh, with a mean contact angle of 29.7°. The most hydrophobic PTh–Ag composites were also observed in this zone with contact angles of 120°, $x \approx 0.45$ and roughness of 25 nm (Rrms). However, for $x>0.45$, the contact angles diminish while the roughness grows notably.

The effect of roughness on contact angles has been explained by Cassie and Baxter [20]. Their assumption was that the liquid may not fill the surface cavities creating air pockets, which results in solid–air–liquid interfaces. Consequently, the increase in roughness in those cases enhances the hydrophobicity of the surface.

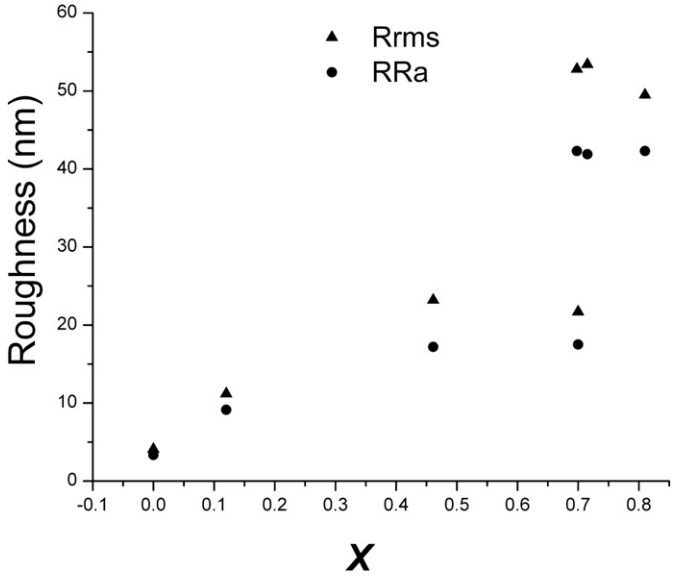

Fig. 7. Roughness as a function of the metallic fraction. The roughness increases slightly from $x=0$ to $x \approx 0.65$. For $x>0.65$, the roughness growth is notable.

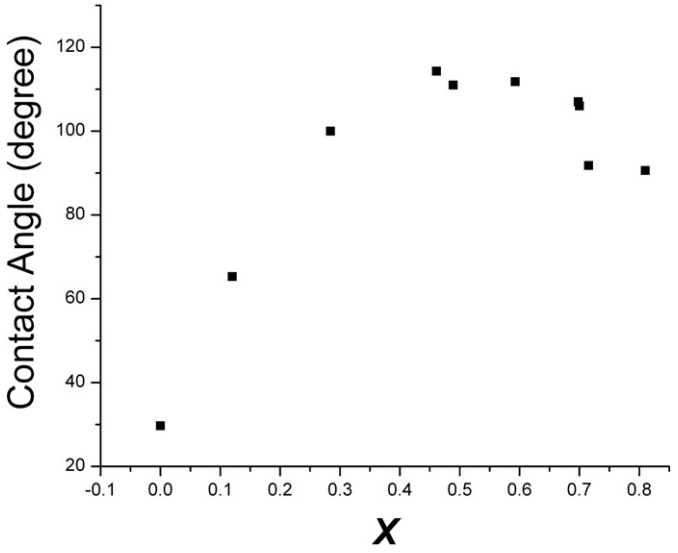

Fig. 8. Contact angle as a function of x, where an almost linear growth of θ, from $x=0$ to $x=0.47$, can be observed.

Based on models and experiments, it has been shown that surfaces with nanotextures [14] and microtextures or their combination [21] are required to form ultra hydrophobic surfaces. In this case, smooth surfaces present the smallest contact angles and nanotextured surfaces present the highest contact angles. The model of Cassie and Baxter predicts a linear relation between the cosine of the contact angle and the fraction of the solid surface area in contact with liquid, f, in the form of $f = \frac{1+\cos\theta}{1+\cos\theta_s}$. If a contact angle, $\theta_s = 29.7°$, is associated with a smooth polymer matrix, namely $f=1$, a value of $f=0.26$ will be enough to reach a contact angle of 120°. This may explain the initial increase of contact angles while the roughness grows. However, the solid surface of the solid–air–liquid interface of the Cassie and Baxter approach in PTh–Ag is made of polymer and metal, and the roughness is a necessary but not a sufficient condition to form water repellent surfaces, because there are other variables that influence the wettability of surfaces. One of these can be a physical coordination between polythiophene, metallic particles and liquids. The distribution of electrical charges in Ag, should affect the polarization in the other components. This coordination has a stage of saturation in the contact angles with respect to the metallic content. Owens and Wendt [22] developed a method to resolve the surface energy into contributions from dispersion and polar bonding forces. This method requires the use of at least two liquids with known dispersive and polar contributions; however, a qualitative description of the dispersive contribution can be found in Fig. 8. Using the equation of Owens and Wendt, with dispersive and polar contributions for water $\gamma_l^d = 21.8$ and $\gamma_l^p = 51.0$ mN/m, respectively: $1+\cos\theta = 0.128\sqrt{\gamma_s^d} + 0.196\sqrt{\gamma_s^p}$ and neglecting changes in the polar contribution, the dispersive contribution could be associated with changes in θ, as predicted by the model of Fowkes. In this way, if γ_s^p was neglected, an increase in θ provokes an abrupt decrease in γ_s^d, from 213 mN/m (29.7°) to 15.2 mN/m (120°). Due to the θ reduction from $x>0.4$, it is reasonable to assume that the effect of metal on the surface energy in PTh matrixes increases the surface energy of the PTh–Ag composites [13], and consequently, the contact angles are reduced. Considering the rule of mixtures, from $x>0.45$, the contribution of the metal on θ becomes more significant than the effect of roughness, which is initially the dominant factor in the PTh–Ag wettability, but as x increases, the chemical properties of the surface become more important. In this way, it is possible to synthesize composites with controlled electrical conductivity and wettability for specific applications.

5. Conclusions

Thin films of PTh–Ag composites were synthesized using DC glow discharges with a filler range from 0 to 0.81 and thickness from 0.3 to 1.3 μm. The electrical field applied to the system promoted the polymerization of the monomer and the ablation of the metallic electrodes, releasing Ag and Cu particles that incorporate into the polymers in progress. As the mass fraction of the metallic components was 90% Ag and 10% Cu, the more intense reflections of Cu in 43.4° and 50.5° were hidden by the Ag reflections.

Metallic particles from 11 nm to less than 1 μm in diameter were obtained. The Ag filler particles presented a preferred orientation of the (111) planes. The percolation threshold was obtained at $x_p \approx 0.12$, lower than the value predicted by the percolation power laws. The composites with metallic nanoparticles changed their thermally activated conduction mechanism at a low critical metal volume of $x_c \approx 0.18$.

The PTh–Ag thin film composites could be varied from hydrophilic to highly hydrophobic by controlling their superficial roughness and metallic content. The superficial nanotexture enhanced the hydrophobicity of the composites. The most hydrophilic material ($\theta = 29.7°$) was PTh with smooth surfaces (Rrms ≈ 4.1 nm) and the most hydrophobic ($\theta = 120°$) was a PTh–Ag composite with nanotexture (Rrms ≈ 23.2 nm) and $x = 0.46$. The results suggested that the metallic particles increased the dispersive interaction of the surfaces and diminished the contact angles. Finally, this work extends the possibility of synthesizing polymer–metal composites with controlled electrical conductivity and wettability for specific applications.

Acknowledgments

The authors acknowledge Carlos Flores-Morales for the AFM and TEM measurements and Araceli Ordóñez-Medrano for the facilities in the contact angle measurements. J. C. Palacios acknowledges CONACyT for his postdoctoral grant.

References

[1] Y. Liu, T. Cui, K. Varahramyan, Solid-State Electronics 47 (2003) 101–104.
[2] P. Santhosh, A. Gopalana, L. Kwang-Pill, Journal of Catalysis 238 (2006) 177–185.
[3] V. Saxena, V.S. Shirodkar, Journal of Applied Polymer Science 77 (2000) 1051–1055.
[4] F. Raymond, N. Di Césare, M. Belletête, G. Durocher, M. Leclerc, Advanced Materials 10 (8) (1998) 599–602.
[5] P. Bäuerie, A. Emge, Advanced Materials 3 (4) (1998) 324–330.
[6] G.J. Cruz, J. Morales, R. Olayo, Thin Solid Films 342 (1999) 119–126.
[7] J. Morales, M.G. Olayo, G.J. Cruz, M. Castillo-Ortega, R. Olayo, Journal of Polymer Science, Part B, Polymer Physics 38 (2000) 3247–3255.
[8] M.G. Olayo, J. Morales, G.J. Cruz, R. Olayo, E. Ordóñez, S.R. Barocio, Journal of Polymer Science, Part B, Polymer Physics 39-1 (2001) 175–183.
[9] G.J. Cruz, J. Morales, M. Castillo-Ortega, R. Olayo, Synthetic Metals 88 (1997) 213–218.
[10] M. Vasquez, G.J. Cruz, M.G. Olayo, T. Timoshina, J. Morales, R. Olayo, Polymer 47 (2006) 7864–7870.
[11] J.C. Palacios, M.G. Olayo, G.J. Cruz, J. Morales, R. Olayo, International Journal of Polymeric Materials 51 (2002) 529–536.
[12] G.J. Cruz, J.C. Palacios, M.G. Olayo, J. Morales, R. Olayo, Journal of Applied Polymer Science 93 (2004) 1031–1036.
[13] R.K. Fu, Y.F. Mei, G.J. Wan, G.G. Siu, P.K. Chu, Y.X. Huang, X.B. Tian, S.Q. Yang, J.Y. Chen, Surface Science 573 (2004) 426–432.
[14] K. Teshima, H. Sugimura, Y. Inoue, O. Takai, A. Tacano, Applied Surface Science 244 (2005) 619–622.
[15] C.J. Lee, M.R. Karim, M.S. Lee, Materials Letters 61 (2007) 2675–2678.
[16] M. Sahimi, Applications of Percolation Theory, Taylor & Francis, Great Britain, 1994.
[17] H. Biederman, L. Martinů, D. Slavínská, I. Chudáček, Pure and Applied Chemistry 60 (5) (1988) 607–618.
[18] Xue Qingzhong, European Polymer Journal 40 (2004) 323–327.
[19] A. Kiesow, J.E. Morris, C. Radehaus, A. Heilmann, Journal of Applied Physics 94 (10) (2003) 6988–6990.
[20] A.B. Cassie, S. Baxter, Transactions of the Faraday Society 40 (1944) 546–551.
[21] B. Bhushan, Y.C. Jung, Ultramicroscopy 107 (2007) 1033–1041.
[22] D.K. Owens, R.C. Wendt, Journal of Applied Polymer Science 13 (1969) 1741–1747.